

# Parameters of sensitivity of Fraunhofer lines to changes in the temperature, gas pressure, and microturbulent velocity in the solar photosphere

V.A. Sheminova

Main Astronomical Observatory, National Academy of Sciences of Ukraine  
Zabolotnoho 27, 03689 Kyiv, Ukraine  
E-mail: shem@mao.kiev.ua

## Abstract

Parameters are proposed for measuring the sensitivity of Fraunhofer lines to the physical conditions in the solar atmosphere. The parameters are calculated based on depression response functions in the LTE approximation. The sensitivity of lines to the temperature, gas pressure, and microturbulent velocity depending on the line and atomic parameters is investigated. The greatest relative temperature sensitivity is shown by weak lines, while the greatest absolute sensitivity is displayed by moderate lines of abundant heavy atoms with low ionization and excitation potentials. The excitation potential and line strength are the crucial factors for the temperature sensitivity. The highest pressure sensitivity is observed for moderate lines of light atoms with very high excitation potentials (exceeding 6 eV), and strong photospheric lines ( $8 \text{ pm} < W < 14 \text{ pm}$ ) of heavy atoms are the most responsive to the microturbulent velocity. The sensitivity parameters can be also used to advantage for physical diagnostics of the photosphere when the temperature, pressure, and microturbulent velocity fluctuations are no more than 8%, 50%, and 100%, respectively.

## 1 Introduction

Local changes in the physical conditions in the solar atmosphere can cause substantial changes in the parameters of observed absorption lines. In such a situation, the spectral line is said to respond to the structural inhomogeneities which have appeared in the line formation region, and the stronger is the response, the more sensitive is the line to changes in the medium. Comprehensive information on the sensitivity of lines to different atmospheric parameters is essential for solving many problems in the spectrum analysis. Caccin et al. made a fundamental contribution to the problem – using the sensitivity function [3] and the sensitivity coefficients [4], they evaluated the changes in the central depth, halfwidth, and equivalent width of several spectral lines caused by changes in the temperature and microturbulent velocity. Unfortunately, the authors have not analyzed the line sensitivity measure introduced by them, and the sensitivity coefficients did not find wide use because of apparently cumbersome calculations. When the sensitivity coefficients are calculated, a variation in a model atmosphere parameter requires that the

whole model be recalculated. Besides that it is difficult to measure the line sensitivity, since the atmospheric parameters have a combined effect on the line profile and it is not simple to determine the sensitivity to one of them.

Studying the contribution and response functions, we have concluded that it is possible to determine the line sensitivity through the use of the response functions by calculating a set of sensitivity parameters. This way is much more handy as regards calculations though it also needs much machine time.

The prime objective of this study is to develop a technique for calculating the sensitivity parameters based on the response functions, investigate the sensitivity of lines to different atmospheric parameters, and find a way to separating those lines which are highly sensitive to one of the atmospheric parameters and have a low sensitivity to other parameters.

The first section describes the algorithm for calculating the sensitivity parameters for absorption lines which form under the LTE conditions; the second section presents the results for Fraunhofer lines; the third section deals with the scope for application of the sensitivity parameters to the diagnostics of the photosphere; and in conclusion we give principal inferences and recommendations for choosing the necessary lines.

## 2 Procedure for calculating the sensitivity parameters.

The calculation of line sensitivity parameters is based on the idea of response functions, which has been developed well enough by many authors [1, 2, 5, 14, 15]. The literature on the response functions was briefly reviewed by Demidov [6]. Recall that the response function describes the magnitude of response of a line to a local change in an atmospheric parameter at each point in the atmosphere along the line of sight. It depends on the kind of disturbance and is a function of the wavelength and optical depth. It is called the emission or the depression response function depending on whether it is calculated for an emission or a depression. The function maxima point to the region in the atmosphere where the emerging emission or depression in the line is the most sensitive to variations in the atmospheric parameters.

To estimate the sensitivity of absorption lines, we have chosen the depression response functions proposed for the first time in [13]. A variation in the observed line depression,  $\delta R$ , which results from a local disturbance of some atmospheric parameter is determined as [13]

$$\delta R(\Delta\lambda) = \int_{-\infty}^{+\infty} RF_{R,\beta}(x, \Delta\lambda) \frac{\delta\beta(x)}{\beta(x)} dx. \quad (1)$$

Here  $R = (I_c - I_l)/I_c$  is the line depression;  $RF_{R,\beta}$  is the response function of the depression;  $\beta$  is the atmospheric parameter which undergoes the disturbance  $\delta\beta/\beta$ ;  $x$  is the optical depth in the logarithmic scale ( $x = \log \tau_5$  where  $\tau_5$  is the optical depth at the wavelength  $\lambda = 500$  nm);  $\Delta\lambda$  is the distance to the line center. If  $\delta\beta/\beta$  is not zero in a thin layer  $\delta x$  in the atmosphere close to the depth  $x$ , the following approximate equality is true for the depression response function:

$$RF_{R,\beta}(x, \Delta\lambda) \delta x \approx \frac{\delta R(x, \Delta\lambda)}{\delta\beta(x)/\beta(x)}. \quad (2)$$

It follows from (1) and (2) that the response function defines the rate of variation in the line depression  $R(x, \Delta\lambda)$  at every point  $x$  in the atmosphere relative to the rate of

variation in the parameter  $\beta$  which undergoes the local disturbance  $\delta\beta/\beta$ . If we integrate the response function with respect to  $x$  and divide it by the value of the “emerging” depression  $R(\Delta\lambda)$ , we obtain a dimensionless quantity which is a variation in the observed depression,  $\delta R/R$ , relative to the local variation  $\delta\beta/\beta$ . We denote this quantity by  $P_{R,\beta}$  and call it the parameter, or the indicator, of the line depression sensitivity. It is calculated with the expression

$$P_{R,\beta}(\Delta\lambda) = \frac{1}{R(\Delta\lambda)} \int_{-\infty}^{+\infty} RF_{R,\beta}(x, \Delta\lambda) dx. \quad (3)$$

As  $\delta\beta/\beta$  in (1) is always taken positive, the sign of the sensitivity parameter corresponds to the sign of  $\delta R(\Delta\lambda)$ . It should be remembered therefore: if the sensitivity parameter  $P_{R,\beta}$  is positive, the depression  $R$  is growing when  $\beta$  increases by  $\delta\beta$ , and if  $P_{R,\beta}$  is negative,  $R$  is diminishing. By analogy with (3), we may define the sensitivity indicator for the line equivalent width:

$$P_{W,\beta} = \frac{1}{W} \int_{-\infty}^{+\infty} RF_{W,\beta}(x) dx, \quad (4)$$

where  $RF_{W,\beta}$  is the integral response function. According to [13], it has the form

$$RF_{W,\beta}(x) = \int_{line} RF_{R,\beta}(x, \Delta\lambda) d(\Delta\lambda). \quad (5)$$

To calculate the sensitivity parameters with (3), (4), we have first to calculate reliably the depression response functions. For the LTE photospheric lines, the expression for the depression response function proposed in [13] may be used:

$$RF_{R,\beta}(x, \Delta\lambda) = \beta \mu^{-1} \ln 10 \tau_5 \frac{\kappa_R}{\kappa_5} \left[ \frac{dS_R}{d\beta} - \frac{1}{\kappa_R} (R - S_R) \frac{d\kappa_R}{d\beta} \right] \exp \left( -\frac{\tau_R}{\mu} \right), \quad (6)$$

where

$$\kappa_R = \kappa_l + \kappa_c \frac{B}{I_c}; \quad S_R = \left( 1 - \frac{B}{I_c} \right) / \left( 1 + \frac{\kappa_c B}{\kappa_l I_c} \right); \quad R = 1 - \frac{I_l}{I_c};$$

$$I_{c,l}(\tau_{c,l}) = \exp \left( \frac{\tau_{c,l}}{\mu} \right) \int_{\tau_{c,l}}^{\infty} \frac{B}{\mu} \exp \left( -\frac{t}{\mu} \right) dt; \quad \tau_R = \tau_l + \int_0^{\tau_c} \frac{B}{I_c} dt.$$

Here  $\mu = \cos \theta$ ;  $\kappa_l$ ,  $\kappa_c$  and  $\tau_l$ ,  $\tau_c$  are the absorption coefficients and optical depths in the line ( $l$ ) and in the continuum ( $c$ );  $B$  is the Planck function.

Since the response function depends on the kind of disturbance, i.e., on  $\beta$ , it is necessary to calculate the response function for each atmospheric parameter whose effect on the line profile we want to estimate. Let the temperature variation  $\delta T/T$  occur in the solar atmosphere, then the depression function of the response to this temperature variation, according to (6), is

$$RF_{R,T}(x, \Delta\lambda) = T \mu^{-1} \ln 10 \tau_5 \frac{\kappa_R}{\kappa_5} \left[ \frac{dS_R}{dT} - \frac{1}{\kappa_R} (R - S_R) \frac{d\kappa_R}{dT} \right] \exp \left( -\frac{\tau_R}{\mu} \right). \quad (7)$$

Similarly we get the expressions for the depression functions of the response to the variations in the gas pressure,  $\delta P/P$ ,

$$RF_{R,P}(x, \Delta\lambda) = P \mu^{-1} \ln 10 \tau_5 \frac{\kappa_R}{\kappa_5} \left[ \frac{dS_R}{dP} - \frac{1}{\kappa_R} (R - S_R) \frac{d\kappa_R}{dP} \right] \exp \left( -\frac{\tau_R}{\mu} \right), \quad (8)$$

and in the microturbulent velocity,  $\delta V/V$ ,

$$RF_{R,V}(x, \Delta\lambda) = -V^2 \mu^{-1} \ln 10 \tau_5 \frac{\kappa_l}{\kappa_5} \left( \frac{2RT}{m} + V^2 \right)^{-1} \left( \frac{\Delta\lambda}{\Delta\lambda_D H(a, v)} \frac{d[H(a, v)]}{dv} + 1 \right) \times \\ \times \left[ \frac{\kappa_c}{\kappa_R} \left( 1 - \frac{B}{I_c} \right) \frac{B}{I_c} - (R - S_R) \right] \exp \left( -\frac{\tau_R}{\mu} \right). \quad (9)$$

The algorithm for calculating the sensitivity parameters of the Fraunhofer lines is based on formulae (7)–(9). The calculation program is based on the SPANSAT program for the Fraunhofer line calculations [7].

### 3 Calculation and analysis of sensitivity parameters

It is well known that the temperature sensitivity of a line depends on the line excitation potential, the sensitivity decreasing with increasing potential. Just this rule is commonly used by observers when they choose lines. However no investigations have thus far been carried out concerning the line sensitivity to other atmospheric parameters and the dependence of the sensitivity on the line atomic parameters such as the wavelength  $\lambda$ , ionization potential, atomic weight, as well as on the abundance and on the line central depth, equivalent width, and half-width. The employment of the above technique for calculating the line sensitivity parameters allowed us to elucidate the problem.

#### 3.1 Starting data for calculations

We have chosen ten groups of lines from the line list given in [9], so that we might deduce the dependences we are interested in. The first group contains lines of different elements with different excitation potentials from 0 to 9 eV and with central depths close to each other in the range from 0.1 to 0.2. Table 1 gives the starting data for the first-group lines;  $AM$  is the atom mass,  $A$  is the element abundance,  $IP$  is the ionization potential,  $EP$  is the excitation potential;  $R$ ,  $\Delta\lambda_{R/2}$ ,  $W$  are the central depth, half-width, and equivalent width of the line;  $\log \tau_{5,R}$ ,  $\log \tau_{5,R/2}$ ,  $\log \tau_{5,W}$  are the effective optical depths of formation of the line center, of the part of the line profile which corresponds to the half-width, and of the entire line on the average. The results of calculations for the lines in the first group permitted us to find how the line sensitivity parameters depend on the excitation potential, ionization potential, abundance, and atomic weight. The second group comprises the iron lines for finding the dependence of sensitivity parameters on the line wavelength. We have selected five lines with  $EP = 4$  eV,  $R = 0.65$ . The remaining eight groups of lines, which include the Fe I lines only, served for determining the dependence of line sensitivity on the line central depth, half-width, and equivalent width. In each of these eight groups we selected lines with close excitation potentials, namely: 0, 1, 1.5, 2.5, 3, 3.5, 4, 5 eV, with different central depths from 0.05 to 0.8 and equivalent widths from 0.4 to 13 pm. Such a selection of lines permitted a simultaneous investigation of the dependence of line sensitivity on both the line strength and the excitation potential, excluding the effect of the ionization potential, abundance, and atomic weight; we could also obtain the sensitivity indicators for actual lines in the solar spectrum.

We used the model atmosphere HOLMU [10] in the calculations of sensitivity parameters. The data on the oscillator strengths and microturbulent velocity, which varies with

Table 1: Response of Line Central Depths to Gas Pressure Disturbance.

no.	$\lambda$ , nm		$AM$	$A$	$IP$ , eV	$EP$ , eV	$R$	$\log \tau_{5,R}$	$P_{R,T}$	$P_{R,V}$	$P_{R,P}$
1	477.588	C I	12.01	8.65	11.26	7.49	0.138	-0.274	2.24	-0.09	-1.08
2	658.762	C I	12.01	8.65	11.26	8.53	0.083	-0.329	3.44	-0.09	-1.35
3	777.539	O I	16.00	8.90	13.62	9.14	0.249	-0.336	4.06	-0.11	-1.36
4	514.884	Na I	22.99	6.32	5.14	2.10	0.128	-0.884	-6.19	-0.19	-0.13
5	669.603	Al I	26.98	6.49	5.99	3.14	0.263	-1.128	-5.09	-0.14	-0.29
6	462.736	Si I	28.09	7.64	8.15	5.08	0.173	-0.845	-2.94	-0.20	-0.31
7	613.185	Si I	28.09	7.64	8.15	5.61	0.183	-0.928	-2.57	-0.18	-0.49
8	674.163	Si I	28.09	7.64	8.15	5.98	0.101	-0.891	-2.28	-0.22	-0.60
9	567.181	Sc I	44.96	3.06	6.56	1.45	0.110	-1.254	-10.18	-0.28	0.04
10	623.936	Sc I	44.96	3.06	6.56	0.00	0.063	-1.424	-14.70	-0.31	0.15
11	477.826	Ti I	47.90	5.06	6.82	2.24	0.183	-1.139	-8.35	-0.28	0.06
12	546.049	Ti I	47.90	5.06	6.82	0.05	0.107	-1.420	-14.72	-0.32	0.22
13	577.403	Ti I	47.90	5.06	6.82	3.30	0.101	-1.021	-7.62	-0.31	-0.10
14	592.212	Ti I	47.90	5.06	6.82	1.05	0.200	-1.404	-10.55	-0.26	0.03
15	445.777	V I	50.94	4.00	6.74	1.87	0.119	-1.143	-9.10	-0.31	0.15
16	482.745	V I	50.94	4.00	6.74	0.04	0.127	-1.420	-13.44	-0.31	0.25
17	521.412	Cr I	52.00	5.64	6.77	3.37	0.204	-1.052	-6.66	-0.29	-0.09
18	523.896	Cr I	52.00	5.64	6.77	2.71	0.189	-1.122	-7.87	-0.29	-0.02
19	666.108	Cr I	52.00	5.64	6.77	4.19	0.110	-1.010	-6.22	-0.32	-0.27
20	557.702	Fe I	55.85	7.64	7.87	5.03	0.118	-0.944	-5.35	-0.33	-0.26
21	561.135	Fe I	55.85	7.64	7.87	3.63	0.101	-1.077	-7.93	-0.35	-0.07
21	568.024	Fe I	55.85	7.64	7.87	4.19	0.112	-1.025	-6.81	-0.33	-0.14
22	662.502	Fe I	55.85	7.64	7.87	1.01	0.149	-1.521	-12.78	-0.31	0.03
23	673.952	Fe I	55.85	7.64	7.87	1.56	0.108	-1.427	-12.08	-0.33	0.01
24	697.194	Fe I	55.85	7.64	7.87	3.02	0.113	-1.243	-9.25	-0.33	-0.11
25	401.109	Co I	58.93	4.92	7.86	0.10	0.080	-1.454	-14.33	-0.37	0.34
26	459.464	Co I	58.93	4.92	7.86	3.62	0.112	-1.015	-6.76	-0.34	-0.01
27	514.979	Co I	58.93	4.92	7.86	1.73	0.102	-1.313	-10.92	-0.35	0.09
28	611.977	Ni I	58.70	6.22	7.63	4.26	0.107	-1.010	-5.51	-0.34	-0.27
29	522.007	Cu I	63.55	4.10	7.73	3.82	0.158	-1.006	-5.73	-0.35	-0.16
30	636.235	Zn I	65.38	4.60	9.39	5.79	0.192	-0.927	-0.39	-0.25	-0.63
31	412.830	Y I	88.91	2.24	6.22	0.07	0.120	-1.272	-12.52	-0.45	0.34
32	468.780	Zr I	91.22	2.56	6.84	0.73	0.136	-1.351	-12.13	-0.43	0.23

height in the photosphere, were taken from [9]. The van der Waals damping constant was taken with a correction factor of 1.5. The macroturbulent velocity was ignored, since it does not enter the response function calculations. The results of calculations are shown in the figures, and the results for the lines of the first group are given also in Table 1. The sensitivity parameters for the complete list of unblended lines [16] are likely to be published separately in tabulated form.

### 3.2 Temperature sensitivity of lines

We consider changes in the temperature sensitivity of lines as functions of principal atomic parameters. The calculations for lines in the first group confirm that the temperature sensitivity depends on the excitation potential. This is clearly seen in Fig. 1a, where the relation  $P_{R,T}(EP)$  is shown. The dependence of the temperature sensitivity on the sum of excitation and ionization potentials  $EP + IP$  is similar in general terms to the dependence of  $P_{R,T}$  on  $EP$ . Analyzing the data in Fig. 1a and in Table 1, we can draw the following conclusions. Lines of atoms with high abundance and large atomic weight, with low excitation and ionization potentials are the most responsive to temperature. As

Table 1. (continued)

no.	$\Delta\lambda_{R/2}, \text{pm}$	$\log \tau_{5,R/2}$	$P_{R/2,T}$	$P_{R/2,V}$	$P_{R/2,P}$	$W, \text{pm}$	$\log \tau_{5,W}$	$P_{W,T}$	$P_{W,V}$	$P_{W,P}$
1	5.1	-0.147	2.91	0.05	-1.13	1.90	-0.196	2.65	0.01	-1.09
2	7.2	-0.197	3.65	0.03	-1.38	1.70	-0.248	3.60	-0.01	-1.35
3	7.2	-0.207	4.50	0.09	-1.45	2.10	-0.260	4.35	0.01	-1.40
4	3.7	-0.749	-5.94	0.05	-0.10	1.20	-0.793	-6.00	-0.03	-0.10
5	5.0	-0.868	-5.58	0.14	-0.23	3.57	-0.966	-5.35	0.05	-0.23
6	3.4	-0.645	-2.92	0.06	-0.24	1.95	-0.696	-2.90	-0.01	-0.24
7	4.6	-0.706	-2.71	0.08	-0.43	2.57	-0.771	-2.70	0.02	-0.41
8	5.3	-0.684	-2.35	0.01	-0.49	1.65	-0.735	-2.30	-0.04	-0.50
9	3.0	-1.102	-10.73	0.17	0.08	1.37	-1.159	-10.45	0.03	0.07
10	3.1	-1.304	-14.89	0.14	0.16	0.71	-1.352	-14.80	-0.03	0.16
11	2.6	-0.973	-8.85	0.19	0.11	1.57	-1.037	-8.60	0.03	0.10
12	2.7	-1.295	-14.94	0.15	0.23	0.78	-1.341	-14.80	0.00	0.22
13	3.1	-0.888	-7.66	0.14	-0.07	1.02	-0.934	-7.60	0.00	-0.07
14	3.1	-1.214	-11.72	0.20	0.08	1.06	-1.291	-11.15	0.05	0.06
15	2.3	-0.995	-9.45	0.18	0.19	1.19	-1.052	-9.25	0.01	0.17
16	2.4	-1.270	-14.07	0.17	0.28	1.17	-1.330	-13.75	0.00	0.26
17	2.9	-0.869	-7.01	0.18	-0.04	1.65	-0.934	-6.85	0.03	-0.04
18	2.8	-0.956	-8.34	0.19	0.02	1.52	-1.016	-8.10	0.04	0.02
19	3.7	-0.840	-6.28	0.12	-0.20	1.23	-0.893	-6.25	-0.01	-0.20
20	3.1	-0.768	-5.39	0.13	-0.19	1.21	-0.819	-5.35	-0.01	-0.19
21	2.8	-0.948	-8.02	0.17	-0.05	0.90	-0.995	-7.95	-0.01	-0.05
21	2.9	-0.881	-6.94	0.17	-0.11	1.11	-0.930	-6.85	0.01	-0.11
22	3.2	-1.349	-13.64	0.19	0.06	1.39	-1.417	-13.25	0.02	0.05
23	3.2	-1.276	-12.60	0.18	0.03	1.11	-1.334	-12.35	0.01	0.02
24	3.4	-1.096	-9.61	0.18	-0.09	1.00	-1.154	-9.45	-0.00	-0.09
25	1.8	-1.319	-14.42	0.17	0.35	0.52	-1.370	-14.35	-0.01	0.34
26	2.3	-0.872	-6.91	0.23	0.02	1.13	-0.926	-6.85	0.02	0.01
27	2.4	-1.171	-11.26	0.20	0.10	0.94	-1.227	-11.10	0.00	0.10
28	3.1	-0.860	-5.66	0.22	-0.24	1.15	-0.913	-5.60	0.02	-0.24
29	2.6	-0.852	-5.93	0.27	-0.13	1.31	-0.908	-5.85	0.04	-0.14
30	3.6	-0.683	-0.45	0.38	-0.63	2.42	-0.781	-0.50	0.12	-0.60
31	1.7	-1.131	-12.69	0.24	0.35	0.83	-1.184	-12.60	0.01	0.35
32	2.0	-1.180	-12.76	0.27	0.26	0.97	-1.245	-12.45	0.05	0.25

seen in the figure, the excitation potential of the lower level has a dominant role in the temperature sensitivity of the line. Lines with excitation potentials to 2 eV are highly responsive, while those with  $EP$  from  $\approx 5.5$  to  $\approx 7.5$  eV are the least responsive. The sensitivity increases again with a further increase of  $EP$ . It is intriguing that the sign of the temperature sensitivity parameter changes. Absorption lines of light atoms with  $EP \approx 6\text{--}7$  eV become stronger with growing temperature, i.e., their central depths and equivalent widths increase. It should be remarked that in this case their temperature sensitivity, while increasing, still remains low. For instance, for one and the same change in the temperature, lines with  $EP \approx 10$  eV change similarly to lines with  $EP \approx 5.5$  eV, though with the opposite sign.

The wavelength dependence of the temperature sensitivity is shown in Fig. 2a. The sensitivity grows with decreasing wavelength, i.e., there is a tendency for the line temperature sensitivity to grow in the shortwave region and to diminish for longer wavelengths.

The sensitivity parameters for three line characteristics – the central depth, half-width depth, and equivalent width – differ slightly in the case of weak lines. This can be seen from Table 1. The most temperature-sensitive is the half-width depth, less sensitive is the equivalent width, and, finally, the central depth. Now we analyze the dependence of

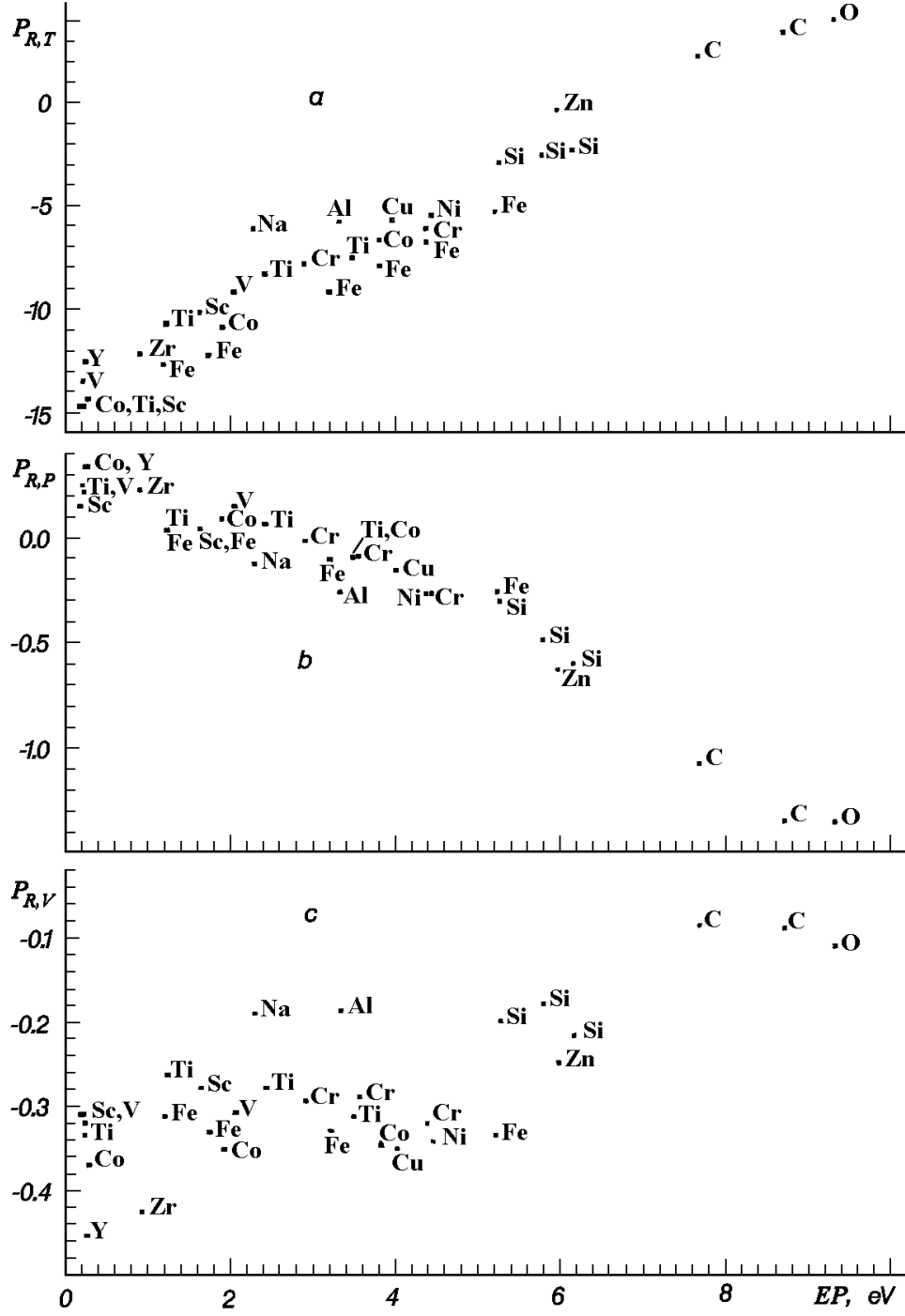


Figure 1: Parameters of sensitivity of the line central depth to temperature (a), gas pressure (b), and microturbulent velocity (c) as functions of the excitation potential.

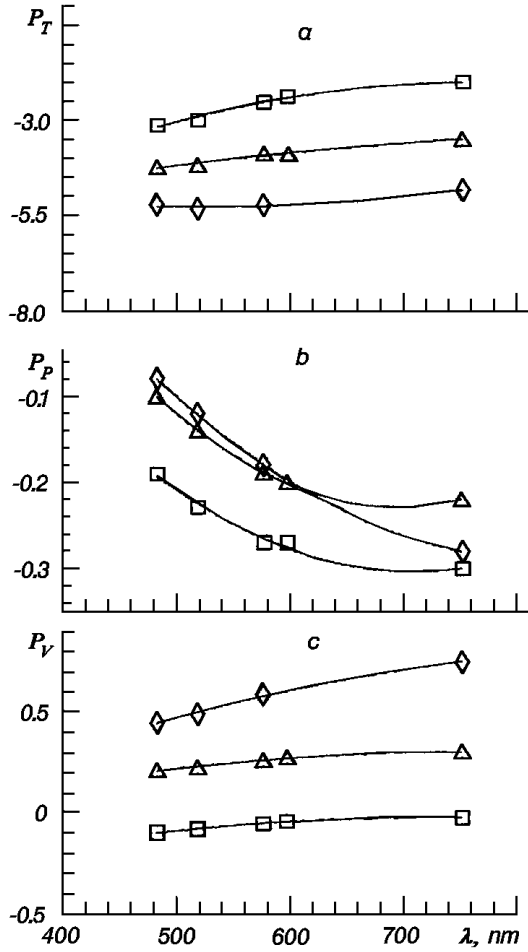


Figure 2: Parameters of sensitivity of the line central depth (squares), half-width depth (diamonds), and equivalent width (triangles) to temperature (a), gas pressure (b), and microturbulent velocity (c) as functions of wavelength.

the line sensitivity on the central depth  $R$ , equivalent width  $W$ , and half-width  $\Delta\lambda_{R/2}$ . Towards this end, we have plotted the relationships  $P_{R,T}-R$  (Fig. 3a),  $P_{W,T}-W$  (Fig. 3b), and  $P_{R/2,T}-\Delta\lambda_{R/2}$  (Fig. 3c) based on the calculations of sensitivity parameters for lines in eight groups. Since the sensitivity depends strongly on  $EP$ , we obtained a family of curves, each curve representing the dependence of the sensitivity parameter on  $R$ , or  $W$ , or  $\Delta\lambda_{R/2}$  for a certain value of  $EP$  in accordance with the calculation results. The figures show the curves for  $EP = 0, 1, 3, 4, 5$  eV only. As it is impossible to choose actual lines in the solar spectrum for each group with the same wavelengths, a small scatter of points can be seen in all figures, which is due to the wavelength dependence of the sensitivity parameters. It is evident from the figures that easily excited weak lines are the most temperature-sensitive. Their sensitivity decreases with increasing  $R$  and  $W$ . Strong lines with high excitation potentials have low sensitivity. The dependence of the sensitivity on the half-width indicates that lines become less sensitive with growing half-width, i.e., narrow lines are more sensitive to the temperature.

Thus, the temperature sensitivity of lines depends the most strongly on the excitation potential above all and to a lesser degree on the line strength. Using the same analysis procedure as for the temperature sensitivity, we studied the sensitivity of lines to the gas pressure and microturbulent velocity.



### 3.3 Sensitivity of lines to the gas pressure

A decisive role in the pressure sensitivity of lines belongs to the low excitation potential. The run of the dependence of line sensitivity to gas pressure on the excitation potential (Fig. 1b) is opposite to that of the sensitivity to temperature. Lines with  $EP$  from 0 to 5 eV have a very low sensitivity to pressure. From 0 to 2 eV, the sensitivity decreases, the central depths and equivalent widths of lines of heavy atoms slightly increasing with pressure. Beginning with 2 eV, lines with higher excitation and ionization potentials and lines belonging to less abundant and lighter atoms become more sensitive to pressure. The most pressure-sensitive lines are those with  $EP > 6$  eV. These may be the lines of carbon, oxygen, nitrogen, as well as lines of ions. Lines of atoms in the iron group may be considered as having low sensitivity to pressure (see Fig. 1b and Table 1). The wavelength also affects the sensitivity of lines to pressure fluctuations. As evident from Fig. 2b, the sensitivity increases with the wavelength, i.e., the effect is opposite to the temperature sensitivity.

The pressure sensitivity depends on the line parameters in a more complicated way than the temperature sensitivity (Fig. 4). A stronger dependence of the pressure sensitivity on  $\lambda$  increases the spread of points on each plot for a certain  $EP$ . The sensitivity grows at first with  $R$  and  $W$  and then diminishes. For instance, the greatest sensitivity of the central part of Fe I lines (Fig. 4a) is observed in those lines for which  $R = 0.4\text{--}0.6$  and  $EP = 5$  eV. When  $EP$  becomes smaller, the maximum sensitivity shifts slightly towards stronger lines. As regards the dependence of the sensitivity on  $W$  (Fig. 4b), the pattern is the same in general. For example, the greatest sensitivity for lines with  $EP = 4$  eV falls within the range of  $W$  from 5 to 7 pm. We can say also that the sensitivity grows at first in the main with the line half-width and then diminishes (Fig. 4c). In contrast to the temperature sensitivity, narrow lines are less sensitive to pressure.

Thus, the greatest response to the gas pressure fluctuations is observed in moderate lines with very high excitation potentials.

### 3.4 Sensitivity of lines to the microturbulent velocity

The analysis of parameters of sensitivity to the microturbulent velocity (Table 1, Figs 1c and 5) reveals that the sensitivity of lines to the microturbulent velocity depends on  $EP$  much more weakly than the temperature and pressure sensitivities. A line is most responsive in the middle part of its wing and least responsive in its central part. For the line central depth, the sensitivity to the microturbulent velocity slightly decreases with increasing  $EP$ , this effect being stronger for stronger lines. The dependence of  $P_{R,V}$  on  $EP$  disappears at all for very strong lines. The the half-width depth, the sensitivity of weak lines remains almost the same with growing  $EP$ , but it increases for strong lines, while for the equivalent width the dependence of  $P_{W,V}$  on  $EP$  is virtually absent. Figure 1c shows how the sensitivity depends on  $EP$  for the central depth. The atomic weight exerts strong control over the sensitivity parameter  $P_{R,V}$ , and we may state that this effect is predominant as compared to other atomic line parameters. It is clearly seen in Fig. 1c how four line groups separate – lines of very heavy atoms (Y, Zr), heavy (Sc, Ti, V, Cr, Mn, Fe, Co, Cu, Zn, Ni), medium-heavy (Na, Mg, Al, Si), and light atoms (C, O). The heavier the atom, the higher the sensitivity of line central part to the microturbulent velocity. The atomic weight affects the sensitivity of the equivalent width to a lesser degree than the sensitivity of the line central part (Table 1). The sensitivity of a line to the microturbulent velocity grows with the line wavelength (Fig. 2c).

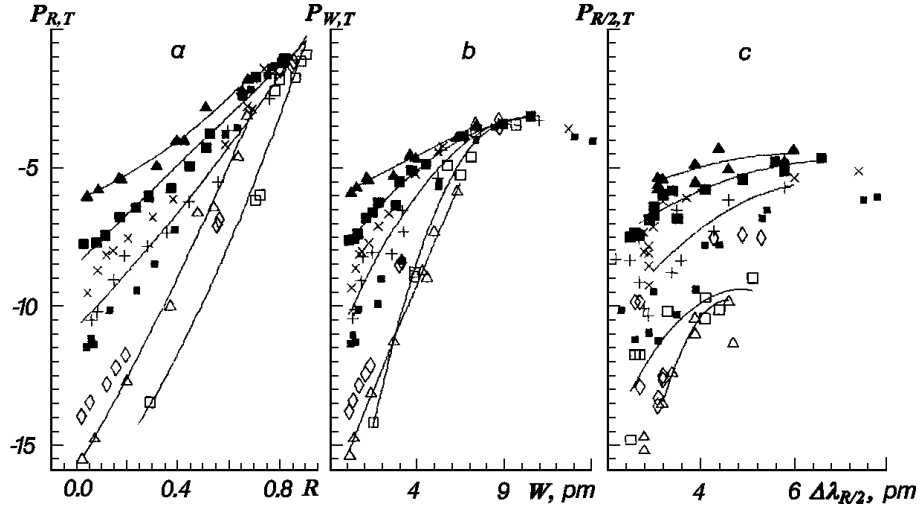


Figure 3: Parameters of sensitivity to temperature for central depth (a), equivalent width (b), and half-width depth (c) as functions of the parameters  $R$ ,  $W$ , and  $\Delta\lambda_{R/2}$ .  $EP = 0$  (light squares), 1 (light triangles), 1.5 (diamonds), 2.5 (dark squares), 3 (plusses), 3.5 (crosses), 4 (big dark squares), 5 (dark triangles). The curves show the dependencies for the lines with  $EP = 0, 1, 3, 4, 5$  eV.

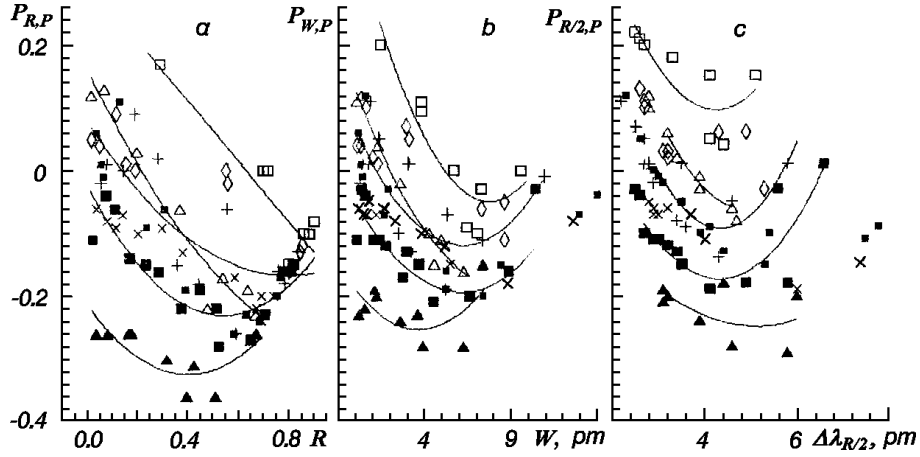


Figure 4: Parameters of sensitivity to the gas pressure. Format is the same as in Fig. 3.

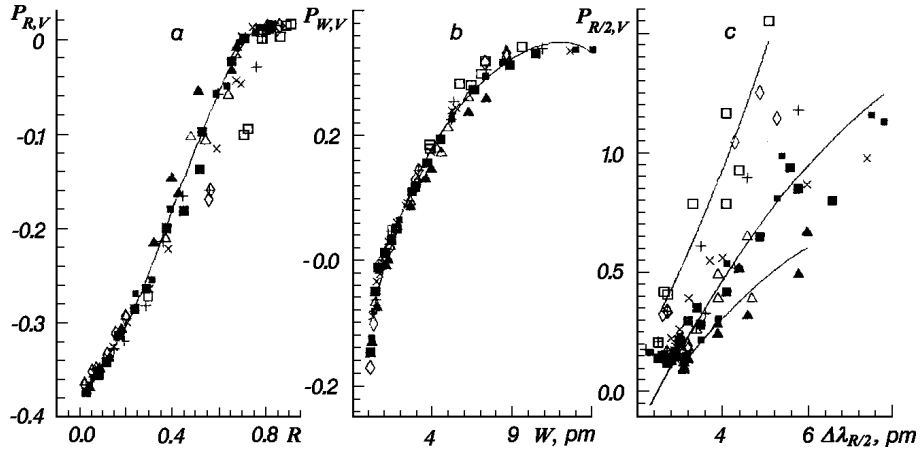


Figure 5: Parameters of sensitivity to the microturbulent velocity. Format is the same as in Fig. 3. The curves show the dependencies for the lines with  $EP = 2.5$  eV (a,b) and  $EP = 0, 2.5, 5$  eV (c).

Figure 5 depicts the line sensitivity as a function of line parameters. The sensitivity of the central depth to the microturbulent velocity decreases quite strongly with increasing  $R$  (Fig. 5a). Lines with  $R \approx 0.7$  are practically insensitive in their central parts. The sensitivity of the equivalent width grows with  $W$  (Fig. 5b), attaining its maximum at  $W \approx 7$  pm, and remains invariant up to  $W \approx 14$  pm, and after that a fall in sensitivity is evident. Figure 5c indicates that wider lines are more sensitive to the microturbulent velocity.

Thus, the sensitivity of a line to the microturbulent velocity is practically independent of atomic parameters. It is governed mainly by the line equivalent width and half-width.

### 3.5 The absolute line sensitivity

We have analyzed the sensitivity of lines, based on the sensitivity indicators calculated with expressions (3)–(4), which characterize a relative variation in line parameters. We call them the relative sensitivity indicators. If we multiply expressions (3), (4) by  $R$  and  $W$ , we can obtain the absolute sensitivity parameters, which characterize absolute depression variations.

We analyzed the absolute sensitivity parameters together with the relative ones. Clearly the dependence of the absolute sensitivity parameters on  $R$  and  $W$  is not the same as shown in Figs 3–5. We shall comment it briefly. If we examine how the absolute sensitivity of central intensities to variations in the atmospheric parameters  $T$ ,  $P$ , and  $V$  depends on  $R$ , we find that moderate lines are the most sensitive, and not weak lines as it was for the relative sensitivity. The maximum absolute temperature sensitivity does not shift for different  $EP$ , it only grows with decreasing  $EP$ . The maximum pressure sensitivity shifts towards smaller  $R$  with increasing  $EP$ , and what is more, it grows. The maximum sensitivity to the microturbulent velocity shifts towards smaller  $R$  and diminishes with increasing  $EP$ . For the absolute sensitivity of equivalent widths, the situation is as follows. The absolute temperature sensitivity increases with  $W$ , this relationship bearing a resemblance to the curve of growth – steeper parts of the curve refer to weak and strong lines, while the flat part refers to moderately strong lines. Depending on  $EP$ , the curve splits into several curves in the region of weak and moderately strong lines. The curves for lines with low  $EP$  lie higher. The dependence of the absolute pressure sensitivity on  $W$  has a maximum for moderate lines which is more clear-cut than in Fig. 4b. The absolute sensitivity to the microturbulent velocity grows linearly with  $W$ , beginning with  $W = 1.5$  pm. The sensitivity does not stop growing for large values of  $W$ .

What sensitivity indicators are better to use for determining line sensitivity – absolute or relative ones? This is likely to depend on the user and the specific problem. It is not difficult to pass from one indicators to other ones. One should know, however, that different lines will have the highest sensitivity (this is especially true for the temperature sensitivity) depending on what sensitivity we bear in mind – the absolute or relative one.

### 3.6 On the scope for application of the sensitivity parameters to the diagnostics of the photosphere

The sensitivity indicators may be also used to determine variations of atmospheric parameters with height. It has been demonstrated with model response functions [11] that the response functions may be used in the spectrum analysis with the aim to determine separately the parameters of the measured solar radiation intensity with a better resolution, even though the response to a disturbance is not always linear and adequate.

Let us consider how appropriate the sensitivity indicators proposed here are for this purpose. First of all, it is necessary to choose correctly the lines, so that deviations of physical parameters from their initial (model) values could be obtained as functions of height with the help of sensitivity parameters from the measurements of observed variations in the line depression. To this end, one has to find lines highly sensitive to a particular atmospheric parameter and at the same time only slightly sensitive to other parameters. Moreover, these lines should be formed at different heights in the photosphere. It is quite easy to find deviations (disturbances in our case) of atmospheric parameters for such a set of lines from the calculated sensitivity parameters. The accuracy of the results lies within the limits defined by the assumptions under which the response functions were derived [5]. Recall that the disturbance should be small and the LTE conditions should be met in the line formation region.

We assume also that the disturbance of an atmospheric parameter occurs throughout the region of the effective line formation. The region of formation of the effective depression extends for photospheric lines over 260–200 km on the average for the line center and 225–150 km for the line wing with  $R = 0.01$  (from the data of [17]). Let the magnitude of disturbance be a certain fraction of the parameter. For example, if this is 5%, then  $\delta\beta = 0.05\beta$  and  $\delta\beta/\beta = 0.05$ , i.e.,  $\delta\beta/\beta = \text{const}$ . Then it follows from (1):

$$\delta R(\Delta\lambda) = \frac{\delta\beta}{\beta} \int_{-\infty}^{+\infty} R F_{R,\beta}(x, \Delta\lambda) dx. \quad (10)$$

Under the adopted assumptions, an relative deviation of the atmospheric parameter from its initial value can be calculated as follows:

$$\frac{\delta\beta}{\beta} = \frac{\delta R(\Delta\lambda)}{R(\Delta\lambda)} \cdot \frac{1}{P_{R,\beta}(\Delta\lambda)}. \quad (11)$$

In this case the line response  $\delta\beta$  always depends linearly on the disturbance magnitude, and there are no difficulties with the nonlinearity and inadequacy pointed to in [11]. Now we determine the limiting values of  $\delta\beta/\beta$  within which expressions (10)–(11) remain true. We calculated directly the central depths of lines using the initial HOLMU model and a set of “disturbed” HOLMU models. The following parameters were taken as independent ones for initial models (all other model parameters were calculated later with them): the geometric height  $H$  of atmospheric layers; temperature  $T(H)$ ; gas pressure  $P(H)$ ; microturbulent velocity  $V(H)$  which was approximated according to [9]:

$$\begin{aligned} V &= \text{const} = 1.08 \text{ km/s}, & H < 130 \text{ km}; \\ V &= \text{const} = 0.55 \text{ km/s}, & H > 420 \text{ km}; \\ V &= 0.946 + H(1.88 \cdot 10^{-3} - 6.75 \cdot 10^{-6}H) \text{ km/s}, & 130 \text{ km} < H < 420 \text{ km}. \end{aligned}$$

To construct the disturbed models, we assumed that one parameter only,  $T$  for instance, varied by  $\Delta T_i = (i/100)T$  due to the disturbance ( $i$  is the disturbance magnitude in percent). Then the new temperature value in the disturbed model becomes  $T_i(H) = T(H) + \Delta T_i(H)$ . Other model parameters are calculated from  $H$ ,  $T_i$ ,  $P$ ,  $V$ . Tables 2–4 give the results of calculations for the variations in the depression at the line center ( $\Delta R_i$ ) arising due to a disturbance of the model parameters  $T$ ,  $P$ , and  $V$ . The first row for each line gives the values of  $\Delta R_i = R - R_i$  obtained from direct calculations of  $R_i$  for a disturbed model and  $R$  for the undisturbed one. The second row gives the values of  $\Delta R$  calculated with the sensitivity parameters from (10). The lines are selected in such a way that their parameters  $EP$ ,  $R$ ,  $P_R$ ,  $\beta$  be as diverse as possible. The last three rows in the

Table 2: Response of line central depths ( $\Delta R_i = R - R_i$ ) to temperature disturbance.  $R$ ,  $R_i$  are line depths calculated for undisturbed and disturbed models,  $i$  is disturbance magnitude in percent.

$\lambda$ , nm	$EP$ , eV	$R$	$\Delta R_1$	$\Delta R_2$	$\Delta R_4$	$\Delta R_6$	$\Delta R_8$	$\Delta R_{10}$	$\Delta R_{15}$	$\Delta R_{20}$
434.723	0.00	0.710	0.050	0.103	0.208	0.303	0.382	0.446	0.552	0.612
Fe I			0.046	0.092	0.183	0.275	0.366	0.458	0.687	0.916
448.974	0.12	0.908	0.009	0.019	0.041	0.066	0.094	0.124	0.208	0.301
Fe I			0.009	0.017	0.035	0.052	0.070	0.087	0.130	0.174
512.767	0.05	0.280	0.038	0.072	0.126	0.165	0.194	0.214	0.244	0.259
Fe I			0.038	0.076	0.153	0.229	0.306	0.382	0.573	0.764
525.020	0.12	0.786	0.020	0.044	0.100	0.167	0.241	0.310	0.465	0.572
Fe I			0.018	0.037	0.074	0.110	0.147	0.184	0.276	0.368
547.316	4.19	0.279	0.018	0.036	0.067	0.093	0.115	0.134	0.169	0.194
Fe I			0.017	0.034	0.068	0.101	0.135	0.169	0.253	0.338
577.845	2.59	0.300	0.027	0.051	0.094	0.130	0.158	0.180	0.219	0.244
Fe I			0.026	0.051	0.103	0.154	0.206	0.257	0.385	0.514
590.567	4.65	0.617	0.018	0.036	0.074	0.111	0.147	0.180	0.253	0.312
Fe I			0.016	0.033	0.066	0.098	0.131	0.164	0.246	0.328
595.669	0.86	0.638	0.034	0.071	0.148	0.223	0.290	0.348	0.452	0.517
Fe I			0.031	0.062	0.125	0.187	0.250	0.312	0.468	0.624
627.022	2.86	0.593	0.024	0.049	0.102	0.153	0.201	0.245	0.332	0.397
Fe I			0.023	0.045	0.091	0.136	0.182	0.227	0.340	0.454
$\Delta_T$	(weak)		0.001	0.002	0.012	0.032	0.060	0.093	0.193	0.306
$\Delta_T$	(moderate)		0.002	0.005	0.014	0.022	0.025	0.023	0.010	0.060
$\Delta_T$	(strong)		0.001	0.006	0.019	0.033	0.045	0.058	0.134	0.212

tables give mean absolute values for the differences  $\Delta_\beta = |\Delta R_i - \delta R|$  separately for weak, moderate, and strong lines.

The analysis of the results reveals that the magnitudes of response calculated directly ( $\Delta R_i$ ) begin to deviate for certain values of  $\delta\beta/\beta$  from the linear dependence of  $\delta R$  on  $\delta\beta/\beta$  obtained with (10). The quantity  $\Delta_\beta$  just characterizes this deviation. When the initial temperature is disturbed, the quantity  $\Delta_T$  increases with the magnitude of disturbance much faster than for the disturbances of the gas pressure or microturbulent velocity. The quantity  $\Delta_T$  depends on the excitation potential and line strength, reaching its lowest value for moderate lines with large  $EP$ . It is evident from Table 2 that the sensitivity parameters may be used for the diagnostics of the solar photosphere when the observed variation  $\delta R$  is no more than  $R/2$  and the disturbance magnitude is no more than 8% ( $\approx 400$  K). There must be no disturbance inversion in the line formation region in this case.

We have somewhat another picture for the gas pressure disturbance. The sensitivity of lines to changes in  $P$  is much smaller, and the quantities  $\Delta_P$  are small, and therefore the sensitivity parameters may be used with confidence for estimating  $\delta R$  or  $\delta P$  when the pressure disturbance is 30% or more. The quantities  $\Delta_V$  for central depths are insignificant at the microturbulent velocity disturbances up to 50%. For equivalent widths,  $\Delta_V$  becomes more significant, being greater for stronger lines. The deviations for strong lines attain 0.13 pm when  $V$  increases by 100%.

If  $\delta\beta/\beta$  depends on height or the disturbance is localized in regions much smaller than the region of formation of the absorption line, the inverse problem cannot be solved, i.e., the quantity  $\delta\beta/\beta$  cannot be determined from the observed  $\delta R/R$  with (11). Formulae (1), (2) should be used in this case.

Now we dwell on the determination of the height where the effective response to the

Table 3: Response of Line Central Depths to Gas Pressure Disturbance.

$\lambda$ , nm	$EP$ , eV	$R$	$\Delta R_1$	$\Delta R_5$	$\Delta R_{10}$	$\Delta R_{15}$	$\Delta R_{20}$	$\Delta R_{30}$
463.407	4.05	0.720	0.002	0.008	0.016	0.023	0.031	0.047
Cr II			0.002	0.012	0.023	0.035	0.046	0.070
505.214	7.68	0.310	0.003	0.011	0.022	0.032	0.042	0.061
C I			0.003	0.014	0.028	0.042	0.056	0.084
525.020	0.12	0.786	0.001	0.004	0.008	0.012	0.017	0.026
Fe I			0.001	0.004	0.008	0.012	0.017	0.026
590.567	4.65	0.617	0.001	0.005	0.009	0.014	0.020	0.030
Fe I			0.002	0.009	0.018	0.026	0.035	0.053
595.669	0.86	0.638	0.000	0.001	0.000	0.001	0.003	0.009
Fe I			0.001	0.006	0.011	0.017	0.022	0.034
624.756	3.89	0.565	0.002	0.010	0.020	0.029	0.038	0.057
Fe II			0.003	0.014	0.028	0.041	0.055	0.083
634.709	8.09	0.407	0.003	0.014	0.027	0.040	0.053	0.077
Si II			0.003	0.016	0.032	0.047	0.063	0.095
777.196	9.14	0.363	0.003	0.012	0.024	0.035	0.046	0.067
O I			0.003	0.014	0.027	0.041	0.055	0.082
789.637	10.00	0.171	0.002	0.009	0.019	0.027	0.036	0.051
Mg II			0.002	0.010	0.020	0.030	0.040	0.060
$\Delta_P$	(weak)		0.000	0.002	0.005	0.006	0.009	0.016
$\Delta_P$	(moderate)		0.001	0.004	0.008	0.012	0.015	0.023
$\Delta_P$	(strong)		0.000	0.003	0.006	0.009	0.012	0.017

Table 4: Response of central depths and equivalent widths of lines to microturbulent velocity disturbance ( $\Delta W_i = W_i - W$ , where  $W$ ,  $W_i$  are equivalent widths calculated for undisturbed and disturbed models,  $i$  is disturbance magnitude in percent)

$\lambda$ , nm	$EP$ , eV	$R$	$W$ , pm	$\Delta R_{30}$	$\Delta R_{50}$	$\Delta R_{100}$	$\Delta W_{10}$	$\Delta W_{30}$	$\Delta W_{50}$	$\Delta W_{100}$
434.723	0.00	0.710	3.753	0.028	0.049	0.100	0.065	0.208	0.336	0.639
Fe I				0.027	0.045	0.090	0.066	0.197	0.329	0.658
438.925	0.05	0.890	7.429	0.002	0.004	0.008	0.244	0.726	1.236	2.592
Fe I				0.002	0.003	0.006	0.236	0.708	1.180	2.360
448.974	0.12	0.908	9.579	0.001	0.002	0.004	0.276	0.872	1.512	3.241
Fe I				0.001	0.002	0.004	0.324	0.972	1.620	3.240
508.334	0.96	0.865	10.768	0.001	0.003	0.006	0.287	0.906	1.577	3.405
Fe I				0.001	0.002	0.004	0.364	1.092	1.820	3.640
512.767	0.05	0.280	1.449	0.024	0.040	0.074	0.006	0.016	0.039	0.069
Fe I				0.025	0.042	0.084	0.006	0.019	0.032	0.063
525.020	0.12	0.786	6.430	0.006	0.010	0.024	0.192	0.562	0.959	1.935
Fe I				0.005	0.009	0.018	0.178	0.534	0.890	1.780
547.316	4.19	0.279	1.743	0.022	0.036	0.068	0.009	0.044	0.061	0.110
Fe I				0.024	0.040	0.080	0.008	0.023	0.039	0.077
577.845	2.59	0.300	1.875	0.024	0.042	0.074	0.011	0.047	0.067	0.120
Fe I				0.025	0.042	0.084	0.011	0.033	0.053	0.112
590.567	4.65	0.617	6.084	0.013	0.022	0.043	0.170	0.408	0.653	1.289
Fe I				0.013	0.022	0.040	0.146	0.438	0.730	1.458
$\Delta_V$	(weak)			0.000	0.002	0.011	0.000	0.013	0.013	0.016
$\Delta_V$	(moderate)			0.000	0.004	0.010	0.001	0.011	0.007	0.019
$\Delta_V$	(strong)			0.000	0.019	0.002	0.034	0.083	0.119	0.130

Table 5: Heights of formation of effective response of lines.

$\lambda, \text{nm}$	$h_R, \text{eV}$	$h_{R,T}$	$h_{R,V}$	$h_{R,P}$	$h_W$	$h_{W,T}$	$h_{W,V}$	$h_{W,P}$
434.723 Fe I	271	240	205	328	232	207	179	228
438.925 Fe I	454	467	484	406	327	227	165	258
448.974 Fe I	560	575	616	513	371	223	156	249
463.407 Fe II	207	178	202	172	146	122	83	106
505.214 C I	59	99	66	53	41	73	35	39
512.767 Fe I	225	222	193	268	208	208	186	247
525.020 Fe I	373	372	342	323	289	233	179	256
547.316 Fe I	147	143	133	96	130	128	121	92
577.845 Fe I	182	178	160	158	165	163	148	155
590.567 Fe I	230	216	214	186	169	142	118	132
595.669 Fe I	289	269	234	235	240	213	178	205
624.756 Fe II	214	222	212	186	158	158	101	129
627.022 Fe I	253	239	219	203	204	181	150	162
634.709 Si I	109	164	121	108	76	111	45	76
777.196 O I	125	183	138	121	86	113	49	86
789.637 Mg II	57	98	63	64	40	61	34	52

line depression variations occurs, resulting from an atmospheric parameter disturbance. This is easy to do with the response functions. One has to find the height at which the center of gravity of the integrand in (1) lies. We have done such calculations for the lines given in Tables 2–4, with the results shown in Table 5, where  $h_{R,\beta}$  and  $h_{W,\beta}$  are the heights of the effective response to variations in  $T$ ,  $P$ , and  $V$  of the line center depression and equivalent width calculated from the depression response functions;  $h_R$  and  $h_W$  are the heights of effective formation of depression at the line center and for the line as a whole, they are calculated from the depression contribution functions. The heights  $h_R$  and  $h_{R,\beta}$ , as well as  $h_W$  and  $h_{W,\beta}$  are obviously different.

To find lines which are the most sensitive to one atmospheric parameter and at the same time have low sensitivity to other parameters, we calculated and compared the relative variations of line parameters,  $\Delta R/R$ ,  $\Delta W/W$ ,  $\Delta R_{\Delta\lambda_{R/2}}/(R/2)$ , rather than sensitivity indicators, for actually observed fluctuations in the temperature (2%), gas pressure (30%), and microturbulent velocity (50%). This way proved to be appropriate for finding the necessary lines. Here we give as an example the wavelengths of typical highly sensitive lines in respect to their relative sensitivity. The most responsive to temperature are the lines 670.778 Li I, 657.279 Ca I, 623.936 Sc I, 546.049 Ti I, 482.745 V I, 511.248 Cr I, 543.253 Mn I, 512.768 Fe I, 662.502 Fe I, 673.952 Fe I, 612.026 Fe I, 635.384 Fe I, 671.032 Fe I, 680.186 Fe I, 685.164 Fe I, 401.109 Co I, 412.830 Y I; the most responsive to gas pressure are the lines 477.588 C I, 505.214 C I, 658.762 C I, 711.317 C I, 833.516 C I, 824.252 N I, 777.196 O I, 777.539 O I, 926.590 O I, 871.783 Mg I, 789.637 Mg II, 875.202 Si I, 634.709 Si II, 891.207 Ca II, 989.070 Ca II, 463.407 Cr II, 463.531 Fe II, 624.756 Fe II; and to microturbulent velocity: 408.295 Mn I, 438.925 Fe I, 448.974 Fe I, 508.334 Fe I, 512.735 Fe I, 514.174 Fe I, 522.553 Fe I, 550.678 Fe I, 625.256 Fe I, 633.534 Fe I, 450.828 Fe II, 402.090 Co I, 508.111 Ni I, 464.866 Ni I, 510.554 Cu I, 481.053 Zn I, 460.733 Sr I, 488.369 Y II, 420.898 Zr II, 455.404 Ba II, 649.691 Ba II.

Analyzing the starting data of these lines and the calculated values of  $\Delta R/R$ ,  $\Delta W/W$ ,  $\Delta R_{\Delta\lambda_{R/2}}/(R/2)$ , we can conclude that the most responsive to temperature are the lines with excitation potentials from 0 to 2 eV, central depths up to 0.35, equivalent widths to 3 pm. Relative variations of the equivalent widths of these lines are 25–30% when the temperature changes by 2%, while they are 2–7% when the gas pressure changes

by 30% and microturbulent velocity by 50%. Moderate-strong lines of light atoms with  $EP \geq 6$  eV are highly responsive to gas pressure. For them,  $\Delta W/W$  is as much as 25–48% when  $P$  changes by 30% and is only 2–6% when  $T$  changes by 2% and  $V$  by 50%. The equivalent widths and half-width depths of strong lines of heavy atoms with  $W \approx 8$ –12 pm and  $\Delta\lambda_{R/2} \approx 4$ –6 pm are very sensitive to the microturbulent velocity. For these lines,  $\Delta W/W$  amounts to 11–18% and  $\Delta(R/2)/(R/2)$  runs as high as 45–70% when  $V$  changes by 50%, and it is 2% when  $P$  changes by 30% and  $T$  by 2%.

## 4 Conclusion

As we could make sure, the sensitivity of every line depends on numerous atom and line parameters as well as on the model atmosphere parameters. It is measured by a diversity of sensitivity indicators with which it is possible to determine the atmospheric parameter producing the strongest response of the line and to estimate the magnitude of the response. It should be taken into consideration which sensitivity, the absolute or relative one, is more suitable for the particular problem. Our calculations reveal that the lines which form under the LTE conditions in the solar atmosphere are the most responsive to temperature variations. Evidence of this is found, for example, in the values of parameters of relative sensitivity to temperature, gas pressure, and microturbulent velocity which attain 15, 1.5, 1.5, respectively (see Table 1). Even minor temperature fluctuations, of the order of 1%, can be observed in the most responsive lines. Fluctuations in the density of matter or in the gas pressure as well as variations in the microturbulent velocity change the line only slightly as compared to temperature. Using the lines most responsive to the gas pressure, it is possible to detect only 10–15% fluctuations of the pressure in the line formation region. Variations in the microturbulent velocity can be measured from variations in the half-widths and equivalent widths of highly sensitive lines if  $\Delta V/V$  is about 30%.

Direct calculations of the response of line depression to variations in atmospheric parameters for disturbed and undisturbed model atmospheres, confirm that the sensitivity indicators can be used for the solar atmosphere diagnostics in those cases when fluctuations in  $T$ ,  $P$ , and  $V$  do not exceed 8%, 50%, and 100%, respectively.

It is better to use the response functions themselves when fine spectral analysis problems are solved. A detailed analysis of the shape of response functions can give an additional valuable information. The results of our analysis show that the sensitivity indicators proposed for measuring the Fraunhofer line response do not lack a physical meaning. We think it reasonable to include the sensitivity parameters in the initial data for spectral lines together with the central depth, equivalent width, and other principal characteristics when the data bases such as “The Fraunhofer Spectrum” [8] are compiled.

**Acknowledgements.** The author thanks V. N. Karpinskii for valuable remarks and useful discussion.

## References

- [1] O. G. Badalyan and V. N. Obridko, “On intensity variations in the photospheric lines and continuous spectrum during small variations in physical parameters,” *Astron. Zhurn.*, vol. 52, no. 3, pp. 561–567, 1975
- [2] J. Beckers and R. Milkey, “The line response function of stellar atmospheres and the effective depth of line formation,” *Solar Phys.*, vol. 43, no. 2, pp. 289–292, 1975.



- [3] B. Caccin, A. Donati-Falchi, and R. Falciani, "Temperature variations in the solar photosphere. I," *ibid.*, vol. 33, no. 1, pp. 49–57, 1973.
- [4] B. Caccin, R. Falciani, and A. Donati-Falchi, "Temperature variations in the solar photosphere. III," *ibid.*, vol. 46, no. 1, pp. 29–52, 1976.
- [5] B. Caccin, N. T. Gomez, C. Marmolino, and G. Severino, "Response function and contribution function of photospheric lines," *Astron. and Astrophys.*, vol. 54, no. 1, pp. 227–231, 1977.
- [6] M. L. Demidov, "Methods for determining depths of formation of Fraunhofer lines. Contribution and response functions," *Issled. po Geomagnetizmu, Aeronomii i Fizike Solntsa*, no. 65, pp. 37–55, 1983.
- [7] A.S. Gadun and V. A. Sheminova, SPANSAT: Program for Calculating Absorption Line Profiles in Stellar Atmospheres in the LTE Approximation [in Russian], Kiev, 1988 (Inst. Theoretical Physics, AS Ukraine Preprint No ITF-88-87P).
- [8] A. S. Gadun, M. M. Sosonkina, and V. A. Sheminova, "The Fraunhofer Solar Spectrum data bank," *Kinematika i Fizika Nebes. Tel* [Kinematics and Physics of Celestial Bodies], vol. 8, no. 2, pp. 80–82, 1992.
- [9] E. A. Gurtovenko and R. I. Kostyk, *The Fraunhofer Spectrum and the System of Solar Oscillator Strengths* [in Russian], Nauk. Dumka, Kiev, 1989.
- [10] H. Holweger and E. A. Muller, "The photospheric barium spectrum: solar abundance and collision broadening of Ba II lines by hydrogen," *Solar Phys.*, vol. 39, no. 1, pp. 19–30, 1974.
- [11] V. N. Karpinskii and N. S. Petrova, *Possibility of the Parametric Resolution of Non-thermal Velocities in the Solar Photosphere* [in Russian], Leningrad, 1989 (VINITI File No 4182-B89).
- [12] E. Landi Degl'Innocenti, "Response functions for magnetic lines," *Astron and Astrophys.*, vol. 56, no. 1/2, pp. 111–115, 1977.
- [13] P. Magain, "Contribution functions and the depth of formation of spectral lines," *Astron. and Astrophys.*, vol. 163, no. 1/2, pp. 135–139, 1986.
- [14] P. Mein, "Inhomogeneities in the solar atmosphere from the Ca II infrared lines," *Solar Phys.*, vol. 20, no. 1, pp. 3–18, 1971.
- [15] F. Q. Orrall, "Intensity fluctuations in Fraunhofer lines," *ibid.*, vol. 23, no. 1, pp. 30–46, 1972.
- [16] R. J. Rutten and E. B. J. van der Zalm, "Revision of solar equivalent widths, Fe I oscillator strengths and the solar iron abundance," *Astron. and Astrophys. Suppl. Ser.*, vol. 55, pp. 143–161, 1984.
- [17] V. A. Sheminova, "Depths of formation of magnetically sensitive absorption lines in the solar atmosphere," *Kinematika i Fizika Nebes. Tel* [Kinematics and Physics of Celestial Bodies], vol. 8, no. 3, pp. 44–62, 1992.